Chinese Journal of Polymer Science Vol. 35, No. 12, (2017), 1540–1551

Chinese Journal of Polymer Science

Temperature-dependent β-Crystal Growth in Isotactic Polypropylene with β-Nucleating Agent after Shear Flow*

Yan-hui Chen[a**], Hao-qing Yang[a], Song Yang[a], Qiu-yu Zhang[a] and Zhong-ming Li[b]
[a] *Department of Applied Chemistry, School of Science, Northwestern Polytechnical University, Xi'an 710072, China*
[b] *College of Polymer Science and Engineering and State Key Laboratory of Polymer Materials Engineering, Sichuan University, Chengdu 610065, China*

Abstract In our current work, the effect of the shear temperature on the growth of β-crystal in isotactic polypropylene (*i*PP) with β-nucleating agent is investigated by means of *in situ* two-dimensional wide-angle X-ray diffraction (2D-WAXD). At low shear temperatures, the formed shear-induced oriented precursors are hard to relax back to random coiled state due to the weak mobility of molecular chains. Therefore, plenty of oriented α-crystals are induced by shear-induced oriented precursors, while β-crystal is greatly depressed. As the shear temperature increases, oriented β-crystal gradually increases along with the decrease of α-crystal. It is deduced that the shear temperature at which the content of β-crystal increases to the (maximum) value found in quiescent crystallization is almost the same as that at which the accelerating effect of flow on crystallization kinetics is completely erased. Our work manifests its significance in regulating β-crystal and thus in the structure and property manipulation of *i*PP.

Keywords Isotactic polypropylene; β-Crystal; Crystallization; Shear temperature

INTRODUCTION

As a polymorphic thermoplastic, isotactic polypropylene (*i*PP) mainly possesses three crystal forms, *i.e.*, monoclinic α-crystal, trigonal β-crystal and orthorhombic γ-crystal[1, 2]. Among these three crystal forms, β-crystal of *i*PP (β-*i*PP) has received a lot of attention in academic research and industrial applications due to its appealing features like excellent impact strength, elongation at break and high thermal deformation temperature[3, 4]. Owing to its thermodynamic metastability, β-crystal can be only obtained under some special conditions, such as temperature gradient[5, 6], application of shear flow[7–9] and addition of a β-nucleating agent[10–13].

For decades, plenty of works have been carried out to investigate the sole influence of β-nucleating agent (*e.g.* type[13] and loading[14]) and shear flow field (*e.g.* shear rate[8] and shear temperature[9]) on the formation of β-crystal. The β-nucleating agent can efficiently induce a great amount of β-crystals by providing numerous heterogeneous β-nucleation sites[15], while shear flow field first orients *i*PP molecular chains to some extent to generate the partially ordered molecular bundles on which β-cylindrites grow epitaxially[16–18]. Both β-nucleating agent and shear flow field demonstrate their efficacy to produce adequate β-crystals. Thus, it is supposed that more β-crystals can be synergistically generated when both factors coexist. Unexpectedly, Varga[19] first pointed

* This work was financially supported by the National Natural Science Foundation of China (Nos. 51473135, 51503170 and 21676217), the Opening State Key Laboratory of Polymer Materials Engineering (Sichuan University) (No. sklpme 2015-4-22) and the Fundamental Research Funds for the Central Universities (No. 3102016BJY01).
** Corresponding author: Yan-hui Chen (陈妍慧), E-mail: yanhuichen@nwpu.edu.cn
Received April 6, 2017; Revised May 15, 2017; Accepted June 2, 2017
doi: 10.1007/s10118-017-1990-x

out that a high shear rate restrained the formation of β-crystal. Huo *et al*.[20] observed that the content of β-crystal consistently decreased as the shear rate increased, indicating a counteraction effect of the shear flow and β-nucleating agent on the formation of β-crystal. To reveal the underlying counteraction mechanism of this intriguing phenomenon, a series of systematic work has been conducted by us[21, 22], which are further utilized to direct the practical processing of *i*PP[23, 24]. In our earlier work, *in situ* synchrotron wide-angle X-ray diffraction (WAXD) and small-angle X-ray scattering (SAXS) measurements were performed to probe the nucleation and growth of α- and β-crystal in β-nucleated *i*PP after shear flow. It was found that at the nucleation stage, the amount of β-nuclei induced by β-nucleating agent and that of α-nuclei created by shear flow and its interaction with β-nucleating agent were at the same order of magnitude; subsequently, at the growth stage, α- and β-crystal grew competitively; as a result, β-crystals were markedly depressed[21]. The growth of α- and β-crystal was later tuned in the practical processing, which endowed *i*PP samples with considerably improved strength and toughness at the same time[24]. An intense shear flow was applied to the outer layer of the sample during the processing, so that the growth of oriented α-crystal overwhelmed its counterpart β-crystal, contributing to the improved strength. On the other hand, the core layer was formed almost under static conditions where shear flow basically decayed and β-nucleating agent functioned properly, thus a high concentration of β-crystals were induced to increase the toughness. To achieve the ultimately optimized properties of *i*PP, the influence of some vital factors on the growth of α- and β-crystal in β-nucleated *i*PP after shear flow needs to be clarified. Higher shear flow rate has already been proved to be disadvantageous for the growth of β-crystal, as it enhances the nucleation of α-nuclei. Introduction of a proper relaxation time after shear flow before cooling down to the crystallization temperature revives not only the content of β-crystal, but also its orientation. Retention time introduced after shear flow is prone to the dissolution of α-nuclei, in other words, promoting the formation of β-nuclei[22].

In this work, the effect of shear temperature on the growth of α- and β-crystal was investigated by means of *in situ* WAXD measurement. It was found that β-crystal was barely formed when the shear temperature was low; as the shear temperature increased, β-crystal gradually revived, simultaneously accompanying with the attenuation of the crystallization kinetics. The underlying mechanism for this intriguing phenomenon was proposed. Our work reveals the effect of shear temperature on tuning the composition of *i*PP samples, paving the way to achieve high-performance *i*PP products.

EXPERIMENTAL

Materials

*i*PP was purchased from Dushanzi Petroleum Chemical Co., Xinjiang, China. The molecular weight $M_w = 3.99 \times 10^5$ g·mol^{-1}, and the polydispersity $M_w/M_n = 4.6$. The melt flow rate was 3 g·(10min)$^{-1}$ (230 °C, 21.6 N). Aryl amide compound (TMB-5) was used as β-nucleating agent (β-NA); its chemical structure is similar to some aromatic amine β-nucleating agents, such as *N*,*N*′-dicyclohexyl-2,6-naphthalenedicarboxamide. This compound was kindly provided by Fine Chemical Institute of Shanxi, Taiyuan, China.

Sample Preparation

β-Nucleating agents were melt-mixed with *i*PP using a twin-screw extruder. The concentration of β-nucleating agent was 0.05 wt%. The screw speed was 82 r·min^{-1}, and the processing temperature window was set between 170 and 180 °C from hopper to die. The extruded pellets were then compressed into films with a thickness of 0.5 mm at 200 °C for 5 min, then air-cooled down to room temperature.

In Situ 2D-WAXD Measurement

In situ two-dimensional wide-angle X-ray diffraction (2D-WAXD) measurement was carried out at the Advanced Polymers Beamline (X27C) in the National Synchrotron Light Source I (NSLSI), Brookhaven National Laboratory (BNL). The wavelength of the X-ray was $\lambda = 0.1371$ nm. A MAR CCD (1024 × 1024 pixels, pixel size = 158.4 μm) was employed to record 2D-WAXD images. The data acquisition time was 20 s for each scattering image. The sample-to-detector distance was 112.9 mm for WAXD (calibrated by

aluminum oxide).

Linear WAXD profiles were obtained from integrating the intensity of 2D-WAXD patterns. Subsequently, the crystallinity (X_c) was calculated using Eq. (1),

$$X_c = \frac{\sum A_{cryst}}{\sum A_{cryst} + \sum A_{amorp}} \tag{1}$$

where A_{cryst} and A_{amorp} are areas of diffraction peaks from crystals and diffused scattering from the amorphous matrix, respectively. When the system consists of both α- and β-crystals, the relative content of the β-crystals (K_β) can be evaluated using the ratio of the area of β-crystal's signature diffraction peak over the total area of major diffraction peaks, given in Eq. (2),

$$K_\beta = \frac{A_\beta(110)}{A_\beta(110) + A_\alpha(110) + A_\alpha(040) + A_\alpha(130)} \tag{2}$$

where $A_\beta(110)$ represents the area of the diffraction peak of (110) for β-crystal; $A_\alpha(110)$, $A_\alpha(040)$, and $A_\alpha(130)$ represent the signature diffraction peaks, namely, (110), (040) and (130), of α-crystal. The crystallinity index of β-crystals (X_β) in this case is given by Eq. (3).

$$X_\beta = K_\beta X_c \tag{3}$$

A Linkam CSS-450 high-temperature shearing stage modified for *in situ* X-ray scattering studies was used to precisely control the shear flow and thermal history of the polymer samples. The temperature and shear conditions used in the 2D-WAXD measurement are shown in Fig. 1. Details of the experimental protocol are as follows: (1) heat the sample quickly from room temperature to 210 °C (after calibration), at a heating rate of 100 K·min^{-1}; (2) hold at 210 °C for 10 min to eliminate residual structures; (3) cool down to a specific shear temperature (150, 160, 170 and 180 °C), at a cooling rate of 30 K·min^{-1} and apply a step shear (the shear rate was 30 s^{-1} with the duration of 10 s); (4) after the shear, cool down the sample to 136 °C at a cooling rate of 30 K·min^{-1}; (5) crystalize the sample at 136 °C. The isothermal crystallization process at 136 °C was monitored using *in situ* 2D-WAXD, as described above. For comparison, quiescent isothermal crystallization (without step shear, denoted as Q) was also conducted.

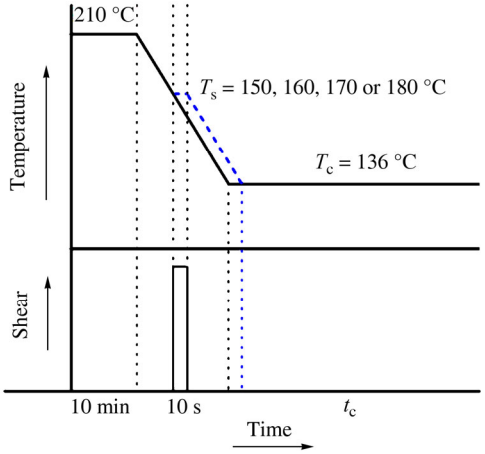

Fig. 1 Schematics of the temperature and shear conditions (step shear 30 s^{-1} for 10 s) as a function of time for *in situ* 2D-WAXD experiment (Shear temperature (T_s) can be 150, 160, 170 or 180 °C.)

RESULTS AND DISCUSSION

A representative series of 2D-WAXD patterns are displayed in Fig. 2, tracing the growth of α- and β-crystal

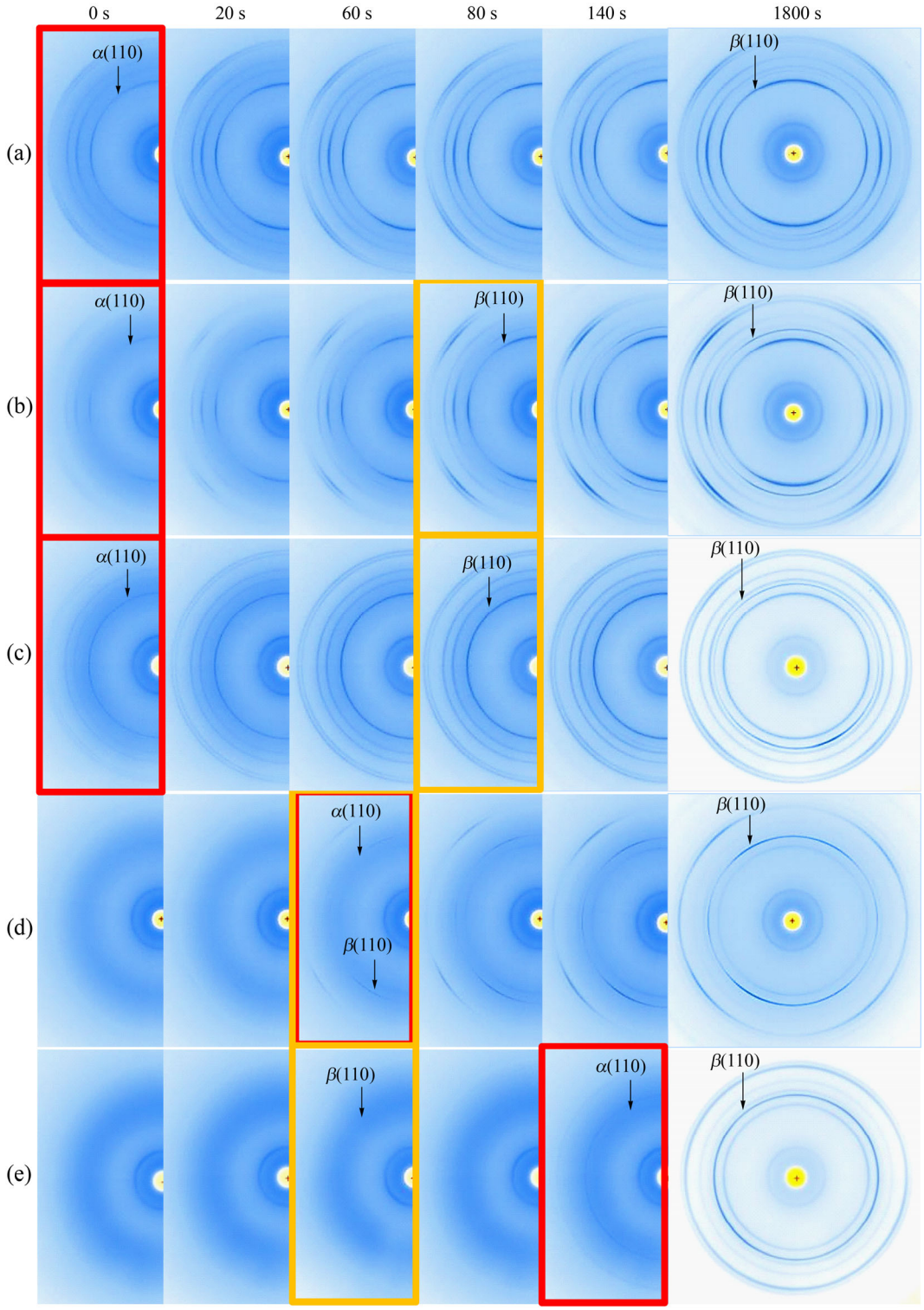

Fig. 2 Selected 2D-WXAD patterns showing the crystal growth of *i*PP with 0.05 wt% β-nucleating agent isothermally crystallized at 136 °C: Shear temperature (a) 150 °C, (b) 160 °C, (c) 170 °C, (d) 180 °C, and (e) quiescent isothermal crystallization without shear (Q)

The shear direction is vertical. The red and yellow rectangles indicate the inception of α- and β-crystals, respectively. The online version is colorful.

when β-nucleated *i*PP samples are isothermally crystallized at 136 °C after the application of shear flow at different temperatures (*i.e.*, 150, 160, 170 and 180 °C). When the shear temperature is 150 °C, α-crystal characteristic lattice planes, that is, α(110), α(040) and α(130), are already present at the onset of crystallization (t = 0 s) and their diffraction gradually intensifies as the isothermal crystallization proceeds. As a result, apparent α-crystal diffraction is observed when the crystallization is completed (t = 1800 s), while β(110) diffraction is very weak. At this low shear temperature, β-nucleation ability of β-nucleating agent is almost depressed by shear flow, so that β-crystal is barely observed. On the contrary, for pure *i*PP sample without β-nucleating agent, plenty of β-crystals are induced by shear flow due to the epitaxial growth of β-crystals on the shear-induced ordered molecular bundles[16–18]. The depression mechanism of β-crystal when β-nucleating agent and shear flow coexisted was fully addressed in our earlier work, attributed to the competitive growth of α- and β-crystal[21]. It can be seen that this low shear temperature (150 °C) is preferred to promote α-nucleation and makes α-crystal grow more competitively than β-crystal, eventually causing the massive reduction of β-crystal. Normally, shear-induced nuclei are considered as a result of the competition between chain relaxation and crystallization[25]. Therefore, this low shear temperature is beneficial for stabilizing chain crystallization to form α-crystal[18].

As the shear temperature increases to 170 °C, the inception of β-crystal is accelerated to 80 s, while α-crystal still emerges at the beginning of crystallization. The elevated shear temperature may stimulate the dissolution of chain orientation and thus decrease α-nuclei. At the same time, the nucleation ability of β-nucleating agent partially revives to promote the occurrence of β-nuclei. The competitive ability of β-crystal is slightly enhanced and its diffraction intensity is relatively strengthened, compared to that of α-crystal. When further elevating the shear temperature to 180 °C, the competitive ability of β-crystal is greatly reinforced. α- and β-crystals simultaneously show up at t = 60 s and β-crystal finally demonstrates obvious diffraction.

The turnover of the appearance of α- and β-crystal happens in the quiescent isothermal crystallization process. β-crystal appears at t = 60 s, earlier than α-crystal. Without shear flow, β-nucleating agent takes full effect to induce the formation of β-crystal. Under such circumstances, the resultant β-crystal dominates in the sample, as evidenced by the highly apparent β(110) diffraction at the end of crystallization.

Besides the diffraction intensity of α- and β-crystal, their azimuthal intensity is also variable. Under the quiescent isothermal crystallization, α- and β-crystals grow homogeneously and do not show any arc-like diffraction. At low shear temperatures (150 and 160 °C), arc-like α-crystal diffraction is present throughout the entire crystallization process, illustrating that the oriented α-crystal was initially induced and maintained till the end of crystallization. At high shear temperatures (170 and 180 °C), α-crystal completely loses its orientation due to the relaxation of chain orientation. However, no matter what the shear temperature is, β-crystal displays noticeable orientation, as shown by the arc-like diffraction of β(110) along the meridian, although its diffraction intensity is relatively low due to its low content at low shear temperatures. Detailed and visualized demonstrations are later presented in Figs. 8–10.

To clearly exhibit the growth of α- and β- crystals as the isothermal crystallization proceeds, linear WAXD curves are ulteriorly presented in Fig. 3. The earlier appearance of α-crystal is observed even when the shear temperature increases to 170 °C; simultaneous appearance of α- and β-crystal happens at 180 °C; β-crystal instead of α-crystal emerges first at the quiescent isothermal crystallization. As the shear temperature increases, the diffraction peak of β(110) becomes higher and higher, compared to that of α(110), indicative of the relative increment of β-crystal. The maximum content of β-crystal is logically achieved in the quiescent β-nucleated *i*PP sample.

To enlighten the effect of shear temperature on the entire crystallization process, normalized relative crystallinity of all β-nucleated *i*PP samples as a function of crystallization time is presented in Fig. 4. The initial crystallinity (t = 0 s) of the sample sheared at 150 °C is as high as 27.3% and reaches the plateau in a short time (t = 450 s). Its half-crystallization time ($t_{0.5}$) is only 37.4 s (Table 1). The continuous rise of the shear temperature reduces the initial crystallinity and in the meantime prolongs the time to reach the equilibrium. In other words, the crystallization rate gradually slows down. The increased shear temperature accelerates the dissolution of

oriented chains, causing the attenuation (150 and 160 °C) and even the disappearance of oriented α-nuclei (170 and 180 °C). Owing to the absence of shear flow, the crystallization rate of β-nucleated *i*PP sample is the slowest under the quiescent condition, where $t_{0.5}$ is equal to 425 s, about eleven times longer than that of the sample sheared at 150 °C. Otherwise, according to 2D-WAXD diffraction patterns and linear WAXD curves, it can be found that the initial contribution to the total crystallinity changes from α-crystal to β-crystal.

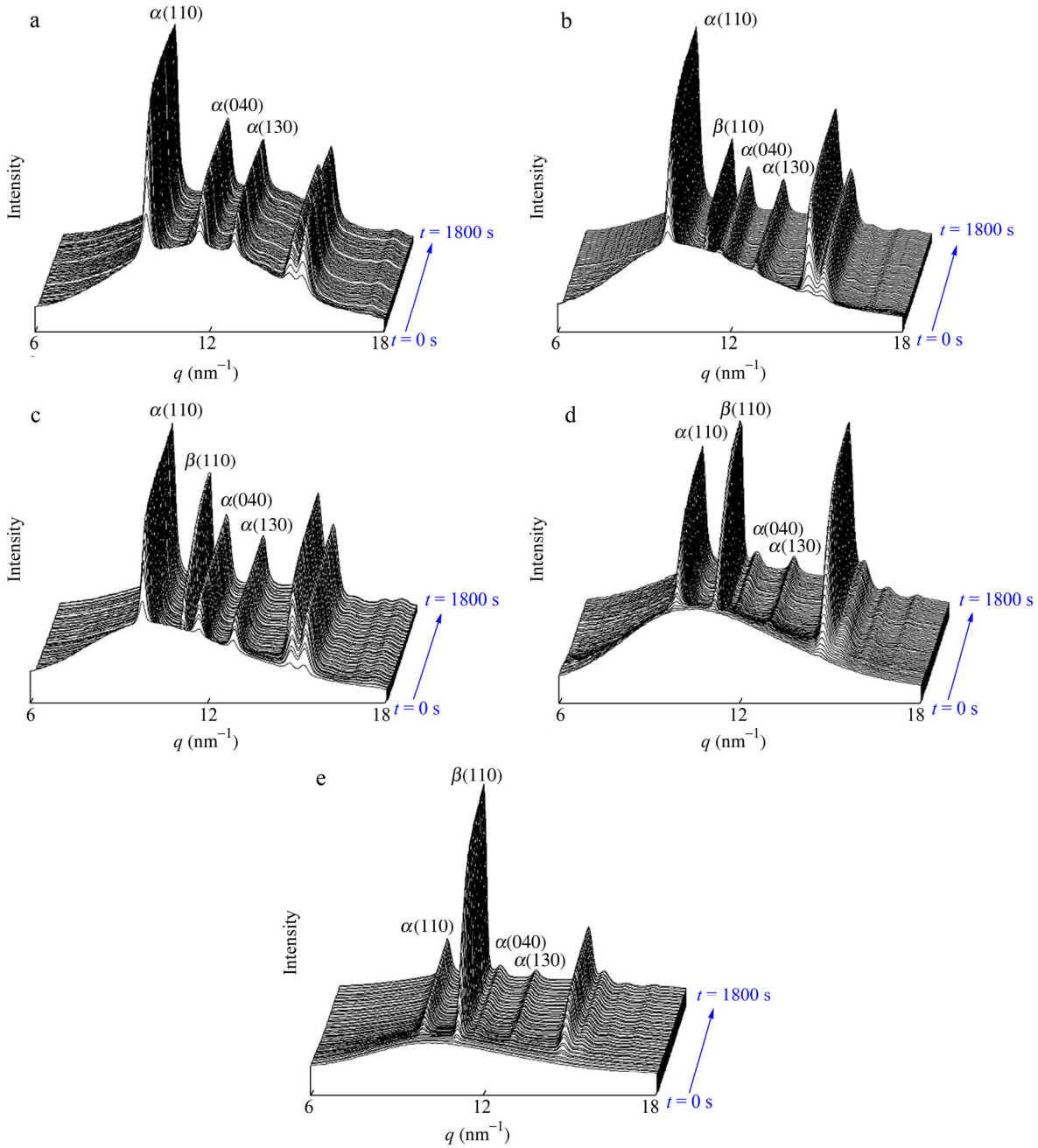

Fig. 3 Linear WAXD intensity profiles as a function of scattering vector (q) of *i*PP with 0.05 wt% β-nucleating agent, obtained from circularly integrated intensities of 2D-WAXD patterns in Fig. 2: (a) 150 °C, (b) 160 °C, (c) 170 °C, (d) 180 °C, and (e) Q

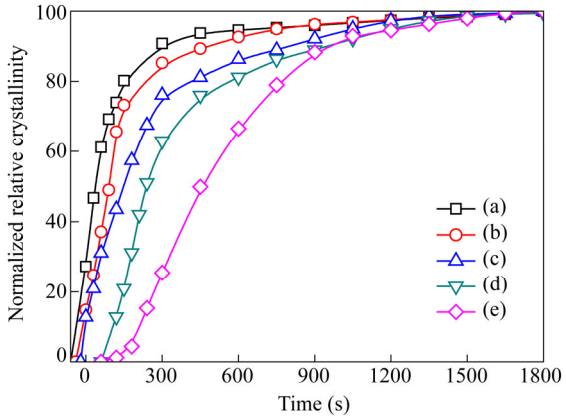

Fig. 4 Normalized relative crystallinity as a function of isothermal crystallization time: (a) 150 °C, (b) 160 °C, (c) 170 °C, (d) 180 °C, and (e) Q

Table 1 Half-crystallization time ($t_{0.5}$) of *i*PP with 0.05 wt% β-nucleating agent when isothermal crystallization at 136 °C is completed

Shear temperature	150 °C	160 °C	170 °C	180 °C	Q
$t_{0.5}$ (s)	37.4	90.4	148.8	412.9	425.0

To quantitatively elucidate the contribution of β-crystal to the total crystallinity, the relative amount of the β-crystals (K_β) and the β-crystal crystallinity (X_β) as a function of isothermal crystallization time are shown in Figs. 5 and 6, respectively. The values of K_β and X_β are approximately equal to zero, confirming the depression effect of low shear temperatures on the formation of β-crystal once again. As the shear temperature increases to 180 °C, the crystallization rate of β-crystal (the slope of the curves) is greatly enhanced, and the resultant K_β and X_β rise to 40.1% and 19.3%, respectively (Table 2). At this shear temperature, the content of β-crystal is still less than that of α-crystal, illustrating that the competitive ability of β-crystal is still weak. The initial K_β is observed to be 100% in the quiescently crystallized β-nucleated *i*PP sample (Fig. 5e), since the original β-crystal rather than α-crystal is induced by β-nucleating agent. Subsequently, K_β largely drops due to the presence of α-crystal. As the crystallization proceeds, the simultaneous growth of α- and β-crystals makes K_β slightly rise. The final K_β and X_β reach 71.7% and 34.9%, respectively (Table 2), being the highest content of β-crystal in all the samples. Compared with other work which conducted the quiescent crystallization of β-nucleated *i*PP sample, the final content of β-crystal is a little bit low[14]. We consider that it may be ascribed to the lower loading of β-nucleating agent (0.05 wt%).

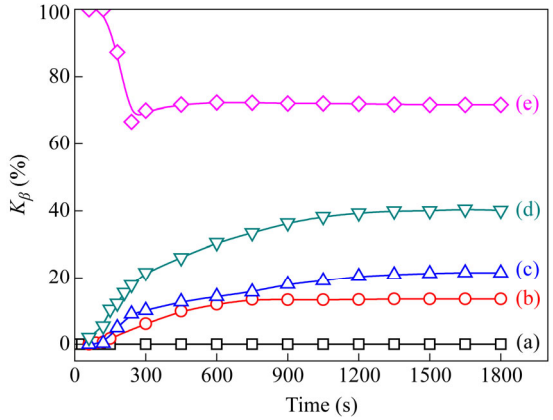

Fig. 5 The relative amount of the β-crystals (K_β) as a function of isothermal crystallization time: (a) 150 °C, (b) 160 °C, (c) 170 °C, (d) 180 °C, and (e) Q

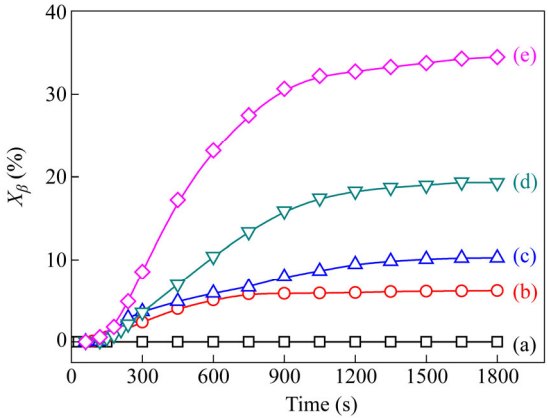

Fig. 6 The β-crystal crystallinity (X_β) as a function of isothermal crystallization time: (a) 150 °C, (b) 160 °C, (c) 170 °C, (d) 180 °C, and (e) Q

Table 2 The final relative amount of the β-crystals (K_β) and β-crystal crystallinity (X_β) of *i*PP with 0.05 wt% β-nucleating agent when isothermal crystallization at 136 °C is completed

Shear temperature	150 °C	160 °C	170 °C	180 °C	Q
K_β (%)	0	13.6	21.5	40.1	71.7
X_β (%)	0	6.5	10.3	19.3	34.9

It is noticed that as the shear temperature increases, the crystallization of β-nucleated *i*PP samples after shear flow progresses with two features: one is the declining whole crystallization rate; the other is the increasing content of β-crystal. To extract the quantitative relationship of these two opposite dynamic processes, two parameters are introduced here: relative shear efficiency (RSE) (Eq. 4) and relative recovery efficiency (RRE) (Eq. 5). As a dimensionless number, RSE, developed by Cavallo *et al.*[26], is related to the residual effect of shear flow on accelerating the crystallization rate:

$$\mathrm{RSE} = \frac{t_{0.5}(T_s) - t_{0.5}(Q)}{t_{0.5}(T_s = 150) - t_{0.5}(Q)} \tag{4}$$

where $t_{0.5}(T_s)$, $t_{0.5}(T_s = 150)$ and $t_{0.5}(Q)$ are the half-crystallization times of samples that have been sheared at different temperatures (150, 160, 170 and 180 °C), sheared at 150 °C and quiescently crystallized (Q), respectively. RSE value ranges from 0 (the absence of shear flow, *i.e.*, quiescent crystallization) to 1 (the maximum shear efficiency, when shear flow is applied at 150 °C). RSE only reflects the effect of the increasing shear temperature on the dissolution (or disappearance) of shear-induced nuclei and does not provide detailed data on their overall concentration.

Analogous to RSE, RRE is proposed here by us to characterize the augment of β-crystals as a result of the increase of the shear temperature[22].

$$\mathrm{RRE} = \frac{K_\beta(T_s) - K_\beta(T_s = 150)}{K_\beta(Q) - K_\beta(T_s = 150)} \tag{5}$$

where $K_\beta(T_s)$, $K_\beta(T_s = 150)$ and $K_\beta(Q)$ are the final relative amount of the β-crystal of samples that have been sheared at different temperatures (150, 160, 170 and 180 °C), sheared at 150 °C and quiescently crystallized (Q), respectively. RRE is equal to 1 when the content of β-crystals reaches its maximum value at the quiescent crystallization; when the shear temperature is 150 °C, RRE is equal to 0, where the content of β-crystal is depressed at its minimum value (*i.e.*, 0). RSE and RRE are then plotted against the shear temperature, as shown in Fig. 7(a). A roughly linear increase of RRE along with an approximately linear decrease of RSE manifests the increment of β-crystal and the deceleration of the crystallization rate, respectively, as the shear temperature increases. The increase of shear temperature does not weaken the shear flow field itself, but impair the effect of shear flow. When the shear temperature is high, the mobility of *i*PP molecular chains is very strong, which makes *i*PP molecular chains hard to be oriented on one hand; on the other hand, the orientation of *i*PP molecular chains is difficult to maintain, even if they are oriented. As a result, shear-induced α-nuclei gradually diminish, accompanying with the resuscitation of β-nuclei. By extrapolating the straight line in Fig. 7(a) to RSE = 0, the shear temperature, at which shear-induced oriented precursors completely vanish (*i.e.*, quiescent crystallization), is estimated to be about 210 °C. Likewise, when RRE extends to 1, it is found that β-crystal content returning to its maximum (*i.e.*, quiescent crystallization) also needs the shear temperature to be about 210 °C. This intriguing phenomenon illustrates that the attenuating rate of crystallization kinetics is basically synchronous with the increasing rate of β-crystal content. Direct evidence is further provided by the plot of RRE against RSE in Fig. 7(b). Based on our previous work, three kinds of nuclei are mainly considered to exist in *i*PP melt when the shear flow is applied to the *i*PP sample with β-nucleating agent, *i.e.*, heterogeneous β-nuclei provided by β-nucleating agent, homogeneous α-nuclei induced by shear flow field and extra α-nuclei created by the interaction between β-nucleating agent and shear flow field. When the shear temperature is high, either homogeneous α-nuclei or extra α-nuclei induced by shear flow are hard to be formed and to be maintained due

to the enhanced mobility of *i*PP molecular chains. As a consequence, the whole content of α-nuclei decreases, leading to the attenuation of crystallization kinetics. On the contrary, β-crystal progressively increases under such circumstances, where its competitive ability is greatly strengthened compared to α-crystal. When the shear temperature increases to 210 °C, shear flow is not able to induce the formation of stable α-nuclei; even if shear flow can induce the formation of some precursors, they will relax to random coiled molecular chains due to the strong mobility of *i*PP molecular chains. Therefore, the whole crystallization rate and the content of β-crystal of samples sheared at 210 °C should be identical to those in the quiescently crystallized samples.

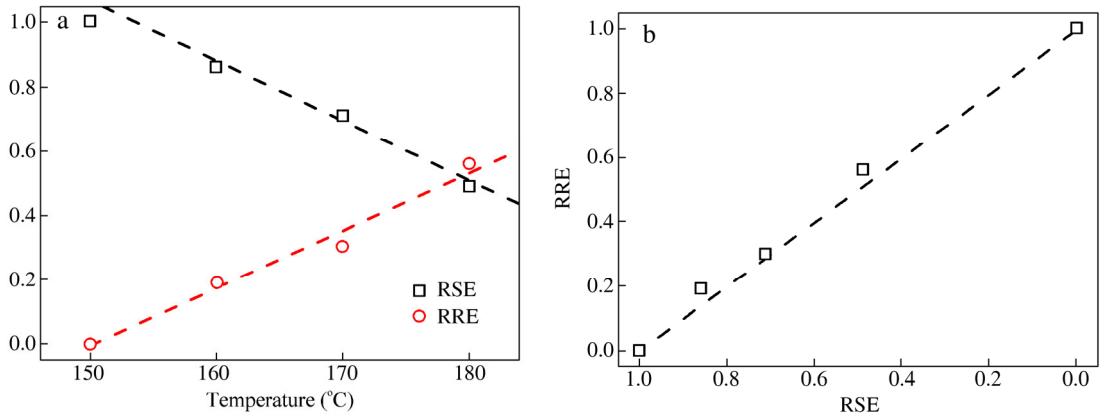

Fig. 7 (a) Relative shear efficiency (RSE) and relative recover efficiency (RRE) as a function of shear temperature; (b) RRE as a function of RSE

The orientation of α- and β-crystals has been initially observed and briefly illuminated in Fig. 2. To reveal the dependence of α- and β-crystals orientation on the shear temperature, the azimuthal diffraction of α(110) and β(110) characteristic lattice planes are extracted from 2D-WAXD patterns in Fig. 2 and shown in Figs. 8 and 9, respectively. The orientation of α-crystal is only clearly observed at low shear temperatures (150 and 160 °C), as evidenced by the diffraction peaks locating at 90° and 270° (at the equator) originated from the parent lamellae of α-crystal and at about ± 10° off the meridian from the daughter lamellae. Once the molecular chains are oriented by shear flow at low temperatures, they are hard to relax back to the initial random state. The subsequent growth of these oriented molecular chains (or shear-induced oriented precursors) gives rise to abundant oriented α-nuclei to induce the formation of oriented α-crystal. As the shear temperature further increases to 170 °C, α-crystal basically does not demonstrate the orientation although the whole crystallization rate is still faster than that in the quiescent condition. In other words, the effect of shear flow on the development of α-crystal orientation is lost much earlier than that on the overall crystallization kinetics. Cavallo *et al.*[26] proposed that the disappearance of shear-induced row-nucleated precursors proceeds through fragmentation at high temperatures, causing the point-like nuclei existing inside the initial shear-induced threadlike structures. Therefore, the crystallization rate is still enhanced even when the orientation of α-crystal is fully lost, which is ascribed to the concentration of point-like nuclei still exceeding the quiescent nucleation density when the shear temperature is high. The critical shear temperature for the disappearance of oriented α-nuclei in our case is 170 °C, while Varga and Karger-Kocsis reported that oriented-nuclei cannot be formed when the shear flow is performed at a temperature higher than 190 °C[16]. This discrepancy may be a result of the different shear rates or the composition of the research system.

Owing to its thermodynamic and mechanical instability, β-crystal is difficult to orient; instead, β-crystal tends to transform into α-crystal (or mesomorphic phase under external forces). In the light of the epitaxial growth of β-crystal on β-nucleating agent, needlelike β-nucleating agent crystals oriented by external forces are able to induce the formation of oriented β-crystal, which have been practically conducted by some researchers[27–31] and us[22, 32]. Normally, β(110) lattice plane of oriented β-crystal demonstrates six well-defined

spots, of which two spots are presented at the equator and four around ± 30° off the meridian[31]. In our case, *β*-orientation is not obvious until the shear temperature reaches 180 °C, as evidenced by its high azimuthal diffraction intensity. It can be concluded that the shear temperature plays an opposite role in the orientation of *α*- and *β*-crystal due to their different orientation mechanism. The *β*-orientation is usually dependent on the morphology of *β*-nucleating agent, which is influenced by the final heating temperature and the loading. It has been previously proved that when treating at 210 °C, *β*-nucleating agent dissolves out in the form of needlelike morphology before *i*PP matrix starts to crystallize[22]. When *β*-nucleated *i*PP is sheared at high temperatures, needlelike *β*-nucleating agent crystals are easily oriented, and hard to regain its initial random state. The addition of *β*-nucleating agent increases the whole system viscosity on one hand; on the other hand, unlike small molecular chains, the mobility of bulky *β*-nucleating agent crystals is quite weak. When the shear temperature is low, it is much harder to orient *β*-nucleating agent crystals due to its further enlarged size and the increased system viscosity. As a consequence, *β*-orientation is weak at low shear temperatures. Detailed explanation about *β*-orientation can refer to our previous work[22].

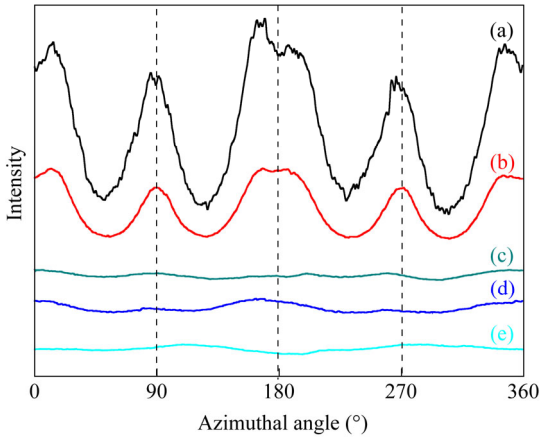

Fig. 8 Azimuthal scan of (110) lattice plane of *α*-crystal on the basis of Fig. 2 when the isothermal crystallization is completed at 136 °C: (a) 150 °C, (b) 160 °C, (c) 170 °C, (d) 180 °C, and (e) Q

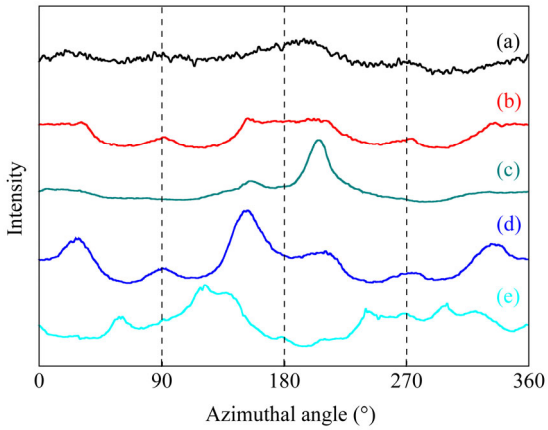

Fig. 9 Azimuthal scan of (110) lattice plane of *β*-crystal on the basis of Fig. 2 when the isothermal crystallization is completed at 136 °C: (a) 150 °C, (b) 160 °C, (c) 170 °C, (d) 180 °C, and (e) Q

A schematic diagram is employed here to illuminate the effect of shear temperature on the growth of *α*- and *β*-crystal and the development of their orientation, as shown in Fig. 10. After the thermal treatment at 210 °C, *β*-nucleating agents completely dissolve in the random coiled *i*PP molecular chains. During the cooling process, bulky needlelike *β*-nucleating agent crystals precipitate first before *i*PP molecular chains start to crystallize. When the shear flow is applied at a high temperature (*i.e.* low degree of supercooling), both of the needlelike *β*-nucleating agent crystals and *i*PP molecular chains are oriented, followed by the intense relaxation of (oriented) ordered *i*PP molecular chains due to the stimulus of high temperature, while the orientation of needlelike *β*-nucleating agent crystals is basically preserved as a consequence of their obviously larger volume. During the isothermal crystallization process, more oriented *β*-heterogeneous nuclei demonstrate a stronger competitive ability compared to *α*-nuclei. Eventually, plenty of oriented *β*-crystals are formed, accompanying with some isotropic *α*-crystals. The situation is totally opposite when the shear temperature is low. At low shear temperatures, shear flow is hard to move bulky needlelike *β*-nucleating agent crystals, but relatively easy to orient *i*PP molecular chains. Under such circumstances, the relaxation of oriented *i*PP molecular chains weakens, so that a great amount of shear-induced *α*-nuclei dominate the following crystal growth at the isothermal crystallization process. As a result, more oriented *α*-crystals are obtained, along with few *β*-spherulites epitaxially growing on the surface of *β*-nucleating agent.

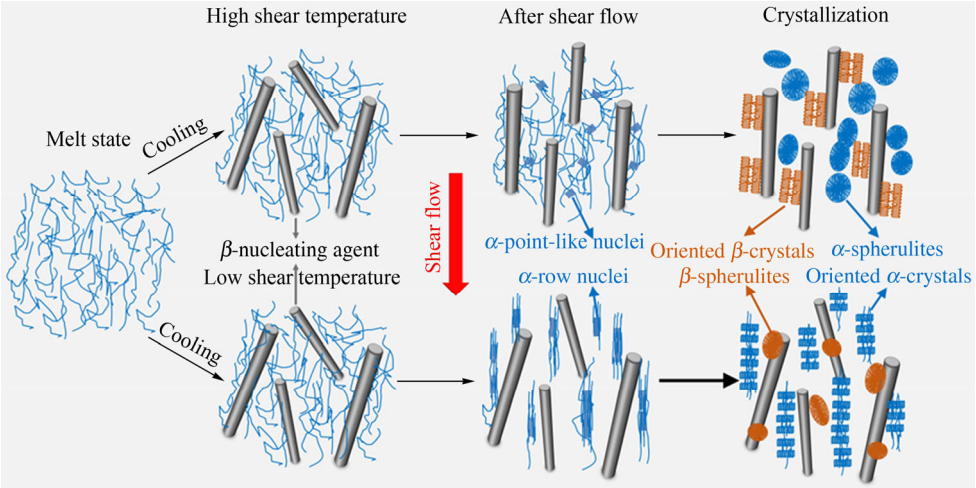

Fig. 10 A schematic diagram of the effect of shear temperature on the crystallization behavior of *i*PP with *β*-nucleating agent after shear flow (The online version is colorful.)

CONCLUSIONS

In this work, *in situ* 2D-WAXD was adopted to trace the growth of *α*- and *β*-crystal after *i*PP with *β*-nucleating agent was sheared at different temperatures. It was found that when the shear temperature was low, oriented *α*-crystal dominated in *β*-nucleated *i*PP samples almost without the presence of *β*-crystal. At higher shear temperature, *β*-crystal content became higher, along with the decease of *α*-crystal. The crystal growth was actually determined by the competitive growth of *α*- and *β*-crystals under different conditions. Higher shear temperature accelerated the relaxation of shear-induced *α*-nuclei and reduced the amount of *α*-nuclei. Therefore, the competitive ability of *β*-crystal was enhanced, giving rise to abundant oriented *β*-crystal at the end of crystallization. The situation was opposite at lower shear temperature. The lower shear temperature weakened the mobility of *i*PP molecular chains and was able to maintain the shear-induced *α*-nuclei, so that oriented *α*-crystal instead of *β*-crystal was predominant in the *β*-nucleated *i*PP samples. In addition, with the increase of shear temperature, the content of *β*-crystals gradually increased, while the overall crystallization kinetics progressively decreased. It is deduced that when the shear temperature is 210 °C, *β*-crystal will increase to the (maximum) value found in quiescent crystallization and simultaneously the effect of flow on crystallization kinetics will vanish. Our work validates the role of competitive growth of *α*- and *β*-crystals proposed by our previous work.

REFERENCES

1 Padden, J.F.J. and Keith, H.D., J. Appl. Phys., 1959, 30(10): 1479
2 Bruckner, S., Meille, S.V., Petraccone, V. and Pirozzi, B., Prog. Polym. Sci., 1991, 16(2-3): 361
3 Varga, J., J. Macromol. Sci. Phys., 2002, B41(4-6): 1121
4 Luo, F., Geng, C.Z., Wang, K., Deng, H., Chen, F., Fu, Q. and Na, B., Macromolecules, 2009, 42(23): 9325
5 Lovinger, A.J., Chua, J.O. and Gryte, C.C., J. Polym. Sci., Part B: Polym. Phys., 1977, 15(4): 641
6 Pawlak, A. and Piorkowska, E., Colloid Polym. Sci., 2001, 279(10): 939
7 Dragaun, H., Hubeny, H. and Muschik, H., J. Polym. Sci., Part B: Polym. Phys., 1977, 15(10): 1779
8 Somani, R.H., Hsiao, B.S., Nogales, A., Fruitwala, H., Srinivas, S. and Tsou, A.H., Macromolecules, 2001, 34(17): 5902
9 Zhang, B., Chen, J.B., Ji, F.F., Zhang, X.L., Zheng, G.Q. and Shen, C.Y., Polymer, 2012, 53(8): 1791
10 Turner-Jones, A. and Cobbold, A.J., J. Polym. Sci. B, Polym. Lett., 1968, 6(8): 539

11 Dong, M., Gu, Z.X., Yu, J. and Su, Z.Q., J. Polym. Sci., Part B: Polym. Phys., 2008, 46(16): 1725
12 Su, Z.Q., Dong, M., Guo, Z.X. and Yu, J., Macromolecules, 2007, 40(12): 4217
13 Wang, J.B., Dou, Q.A., Chen, X.A. and Li, D., J. Polym. Sci., Part B: Polym. Phys., 2008, 46(11): 1067
14 Luo, F., Wang, K., Ning, N., Geng, C., Deng, H., Chen, F., Fu, Q., Qian, Y. and Zheng, D., Polym. Adv. Technol., 2011, 22(12): 2044
15 Zhou, J.J., Liu, J.G., Yan, S.K., Dong, J.Y., Li, L., Chan, C.M. and Schultz, J.M., Polymer, 2005, 46(12): 4077
16 Varga, J. and Karger-Kocsis, J., J. Polym. Sci., Part B: Polym. Phys., 1996, 34(4): 657
17 Sun, X., Li, H., Wang, J. and Yan, S., Macromolecules, 2006, 39(25): 8720
18 Zhang, B., Chen, J.B., Zhang, X.L. and Shen, C.Y., Polymer, 2011, 52(9): 2075
19 Varga, J., J. Therm. Anal. Calorim., 1989, 35(6): 1891
20 Huo, H., Jiang, S.C., An, L.J. and Feng, J.C., Macromolecules, 2004, 37(7): 2478
21 Chen, Y.H., Mao, Y.M., Li, Z.M. and Hsiao, B.S., Macromolecules, 2010, 43(16): 6760
22 Chen, Y.H., Fang, D.F., Lei, J., Li, L.B., Hsiao, B.S. and Li, Z.M., J. Phys. Chem. B, 2015, 119(17): 5716
23 Chen, Y.H., Huang, Z.Y., Li, Z.M., Tang, J.H. and Hsiao, B.S., RSC Adv., 2014, 4(28): 14766
24 Chen, Y.H., Zhong, G.J., Wang, Y., Li, Z.M. and Li, L.B., Macromolecules, 2009, 42(12): 4343
25 Zhao, Y.F., Hayasaka, K., Matsuba, G. and Ito, H., Macromolecules, 2013, 46(1): 172
26 Cavallo, D., Azzurri, F., Balzano, L., Funari, S.S. and Alfonso, G.C., Macromolecules, 2010, 43(22): 9394
27 Li, H.H., Jiang, S.D., Wang, J.J., Wang, D.J. and Yan, S.K., Macromolecules, 2003, 36(8): 2802
28 Phulkerd, P., Hagihara, H., Nobukawa, S., Uchiyama, Y. and Yamaguchi, M., J. Polym. Sci., Part B: Polym. Phys., 2013, 51(11): 897
29 Phulkerd, P., Nobukawa, S., Uchiyama, Y. and Yamaguchi, M., Polymer, 2011, 52(21): 4867
30 Yamaguchi, M., Irie, Y., Phulkerd, P., Hagihara, H., Hirayama, S. and Sasaki, S., Polymer, 2010, 51(25): 5983
31 Yamaguchi, M., Fukui, T., Okamoto, K., Sasaki, S., Uchiyama, Y. and Ueoka, C., Polymer, 2009, 50(6): 1497
32 Chen, Y.H., Yang, S., Yang, H.Q., Zhong, G.J., Fang, D.F., Hsiao, B.S. and Li, Z.M., Polymer, 2016, 84: 254